

# NASA Technical Memorandum 78802

## INITIAL RESULTS OF A POROUS PLUG NOZZLE FOR SUPERSONIC JET NOISE SUPPRESSION

(NASA-TM-78802) INITIAL RESULTS OF A POROUS  
PLUG NOZZLE FOR SUPERSONIC JET NOISE  
SUPPRESSION (NASA) 21 p HC A02/MF A01

N79-13820

CSCI 20A

G3/71 39033

Unclass

Dr. Lucio Maestrello

November 1978

**NASA**  
National Aeronautics and  
Space Administration  
**Langley Research Center**  
Hampton, Virginia 23665





## INITIAL RESULTS OF A POROUS PLUG NOZZLE FOR SUPERSONIC JET NOISE SUPPRESSION

By Lucio Maestrello

### INTRODUCTION

There is continued concern about the noise generated by the exhausts of high performance jet engines such as those required for future supersonic transport type aircraft. The control of shock noise is of particular concern. It involves two components. One component consists of discrete harmonically related tones, often termed screech noise (ref. 1), generated by an acoustic feedback mechanism. The other component is more of a broadband type but is strongly peaked and is known as shock associated noise (refs. 2-4). The shock and shock cells are formed by compression or expansion waves that trail downstream of the nozzle, the results of an imperfectly expanded flow.

As part of a continuing study of possible methods of jet noise reduction, some tests have been made on a porous plug type noise suppressor. Very little information exists in the literature on the aeroacoustic performance of jet nozzles having porous elements designed to eliminate the shock waves in the exhaust stream and by so doing to eliminate the shock associated noise and screech.

The purpose of this paper is to present some initial results on the aeroacoustic performance of a model porous plug type jet noise suppressor. Included are shadowgraph pictures of the flow exhausting from the porous plug nozzle with the comparable acoustic far-field spectra and cross-correlations which illustrate the benefits of the test device.

## APPARATUS AND METHODS

### Description of Test Nozzles

The porous plug nozzle suppressor for which aeroacoustic results are presented herein is shown in the photograph of figure 1. The hollow center body is 7.62 cm in diameter and extends a length of 39 cm from the nozzle exit. It has a surface porosity of about 2 percent (ratio of open area to total area) which was accomplished by drilling a pattern of 0.07 cm radial holes around its periphery. The ratio between the diameter of the center plug and the basic nozzle is 0.833 with a net flow exit area of  $20.27 \text{ cm}^2$  (equivalent to 2.0 inch diameter jet).

The interior cavity of the plug is vented to the jet stream all along its length and acts like a settling chamber whose pressure is nearly equal to ambient. It thus tends to equalize the abrupt positive and negative pressure gradients of the jet stream.

Upstream of the nozzle, the plug cavity was connected through a pipe to a pump which could operate either for blowing or suction. For the present tests, however, forced flow was not used. The planned objective was achieved by either venting the pipe to atmosphere or by closing it off completely.

The extended plug center body may also act as a stabilizer of the jet column because it extends well into the fully developed region such that the secondary jet forms after the flow is at low velocity.

A simple convergent nozzle having an exit diameter of 5.08 cm and having the same open flow exit area as the above porous plug nozzle was also tested to obtain comparable data as a basis for evaluating the aeroacoustic performance of the porous plug nozzle. Both nozzles were tested over a range of pressure ratios between 1.136 - 3.72 and at ambient temperature.

#### Measurements

Two-point space-time correlation measurements of the acoustic pressure were made inside an anechoic chamber about an arc of radius 3.81 m with microphones spaced 5° apart, and located between 20° and 90° from the direction of flow. Fourteen (14) carefully phase-matched microphones were employed (1.27 cm in diameter condenser type). The microphone array was designed such that the microphone distances and angles were accurately controlled. The acoustic pressure was recorded on an FM magnetic tape recorder within the band between 10 Hz to 40 KHz. The data reduction was accomplished using analog means through a playback system. At higher pressure ratios the shock patterns were detected by using shadowgraph techniques.

### EXPERIMENTAL RESULTS AND DISCUSSION

#### Aerodynamic Flow

The shadowgraph pictures of figure 2 illustrate some of the features of operation of the porous plug nozzle. Data for the standard circular

nozzle and for two plug nozzles, all having equivalent open areas and operating at a nozzle pressure ratio of 3.72 are shown in the figure. Note that for convenience each of the photographs is cropped so that only a portion of the flow field is shown.

The flow of the standard convergent nozzle (shown in the top photograph) is underexpanded, a condition favorable for the formation of a pattern of shocks along the jet column. Portions of three shock cells are evident, and others were observed downstream of the portion shown in the photograph. The shocks are weaker further downstream and eventually disappear probably due to turbulent diffusion as the flow becomes subsonic. The shocks observed in the shadowgraphs are believed to be the sources of broadband sound arising from their interactions with convected turbulence. No acoustic feedback was observed at the pressure ratio of 3.72, but was observed for some other pressure ratios.

The flow of the porous plug nozzle (see bottom photograph) is free of shocks and since the mean static pressure balances with ambient, the flow is ideally expanded. The mean Mach number of the jet, therefore, exceeds that of the standard jet for which the flow is not ideally expanded. The elimination of the shocks as illustrated in the bottom photograph has been observed over the entire range of pressure ratios of the tests.

The flow over the nonporous plug as shown in the center photograph, is not free of shocks. A comparison of the results for the porous and

nonporous plugs indicate that the venting holes readjust the pressure gradient in the flow, thus preventing the formation of shocks and shock cells. The presence of a plug (center photograph) changes the inviscid characteristics of the flow in two ways: (1) it changes the flow field from nearly axisymmetric to nearly two dimensional and thus eliminates the intensifications or "focusing" of the compression waves or weak shocks near the axis and, (2) the porosity of the plug (bottom photograph) induces equilibrium in mean static pressure and thus prevents the reflection of the shock waves at the wall of the plug.

#### Acoustic Radiation

The power spectral densities of the far-field sound for the standard nozzle and the porous plug nozzle, at  $90^\circ$  and  $20^\circ$  from the direction of the flow are shown in figures 3 and 4, respectively.

Note that the spectrum for the standard jet at an angle of  $90^\circ$  exhibits a broad peak at a frequency about 7 kHz which is believed to be shock associated noise. This latter component has been shown to radiate significantly between angles of  $60^\circ$  to  $140^\circ$  from the direction of flow, which are important for flyover noise (ref. 5). On the other hand, mixing noise was shown to dominate the spectrum at lower angles (ref. 3). Similar data for the porous plug nozzle indicates no peaks due to shock associated noise. This result is consistent with the shadowgraph data of figure 2 which suggested that the shock waves were completely eliminated in this case.

Note also that the porous plug nozzle spectra indicate noise reductions essentially at all frequencies and at each of the angles. The result suggests that the shear noise component is reduced as well as the shock associated noise component. The reduction of shear noise is a general result since it was observed at subsonic jet pressure ratios as well as at supercritical pressure ratios.

Notice, however, that noise reduction occurs also at the  $20^\circ$  angle (see fig. 4) for which the mixing noise predominates. In fact, significant mixing noise reduction occurs even when the Mach number is subsonic, particularly at small angles from the jet axis. This can be attributed to a reduction in shear noise rather than in self-noise, (see Ribner, ref. 5). In fact, reduction in the thickness of the shear layer effects the lower frequency part of the spectrum because it reduces the scale. This point is covered in the Ribner and Lighthill theories (refs. 5 and 6).

Both shock associated noise and screeching have been observed for a pressure ratio of 3.04 and some example data are shown in figure 5. The screech components are discrete tones superimposed on the broadband shock associated and mixing noise components. Again, one can observe that the spectra for the porous plug nozzle is free of shock noise, because in effect the porous plug prevents shock formation. Consequently, the resulting noise level is considerably reduced. Spectrum for the porous plug is believed to be lower in level than the spectrum of an ideally expanded supersonic jet.

The spatial extent of the sources in the jets can be deduced from the far-field cross correlation measurements shown in figures 6 and 7, with the fixed microphone located at  $90^\circ$ . These figures show the normalized space time cross correlations of the far-field pressure as a function of time delay for various angular separations between  $90^\circ$  and  $70^\circ$ . These correlations were taken at a pressure ratio of 1.45 (jet Mach no  $\approx .74$ ) instead of at 3.72 because the presence of shocks at the higher pressure ratio in the standard jet makes the interpretation difficult. What these figures reveal is that the time delay of the correlation maxima is significantly different between the two nozzles. The porous plug data show that the radiated sound reaches the far-field microphones at about the same instant since the correlation maximum occur near zero time delay. The sources therefore appear to be concentrated within a very narrow region of the shear layer. For the standard jet, on the other hand, they appear to be distributed over a much larger spatial extent since the correlation maxima occur over a range of time delays. For both of these cases, the time delay due to refraction, as well as the contributions due to convection of the mean flow and the source motions are not significant.

The dependence of acoustic intensity on the mean Mach number of the jet ( $M_j$ ) at four different angles from the jet axis, namely  $90^\circ$ ,  $60^\circ$ ,  $40^\circ$ , and  $20^\circ$  is shown in figure 8 for both standard convergent and porous plug nozzles. Included is a reference line faired through the  $90^\circ$  angle data in each case. For the standard nozzle the data are seen to deviate from the faired line at Mach numbers ( $M_j$ ) greater than 1.0 due to the presence of the shocks. On the other hand, for the



plug, the data follow the same trend over the whole operation range, thus indicating shock free flow. There tends to be less intensity level variation at angles between  $20^\circ$  and  $90^\circ$  for the porous plug nozzle than for the standard nozzle. This is an indication that the noise sources of the porous plug nozzle are concentrated in a small region of the flow and that the directivity pattern is more uniform than that of the standard jet.

The results of measurements in reference 7 for a jet exhausting through a wire grid show a nondirectional radiation pattern similar to that of the porous plug nozzle as well as a reduction in amplitude in the lower frequency part of the spectrum as shown in figure 4. The flow velocity profiles in the plug nozzle and in a jet exhausting through a wire grid are quite different, because the former is being narrowed and the latter is being broadened with respect to a standard jet. However, the thickness of the shear layer between the minimum and the maximum velocities is relatively small in both cases, compared to that of a standard jet. This narrowing of the shear layer is believed to account for the shear noise reduction because it reduces the spatial scale of the large structure of the flow.

Because of the highly localized field of the sources in the porous plug nozzle there is the possibility of further noise reductions by means of shielding. In order to investigate this possibility a test was conducted using an acoustic shield or baffle and the results are given in figure 9. The baffle consists of a 10 cm thick polyurethane

blanket, placed about 30 cm away from the jet, curved over a  $90^\circ$  arc, and inclined  $15^\circ$  away from the direction of the flow. The use of this acoustic baffle has produced the noise reductions shown in the figure for a measurement angle of  $90^\circ$ . The attenuation is significant for frequencies above 1 KHz, while at lower frequencies, there is a small increase in noise level. Similar results were obtained at all angles and pressure ratios of the tests. The consistent increase in noise levels at low frequencies for all tests with the baffle is not completely understood but it is however consistent with past experience of operating jets in close proximity to surfaces.

#### Thrust Performance

Determinations of the jet total thrust were made by measuring the force of a jet impinging on a large thick plate mounted at 95 cm downstream of the nozzle. The jet impinged on one-half of the plate and exerted a force on the load cell on which the other half of the plate rested. The ratio between the thrust of the standard jet and that of the porous plug nozzle was obtained by the ratio of the voltage outputs from the load cell. This ratio was about 0.99 at a pressure ratio of 3.72. At lower pressures it decreased to 0.96 at the lowest subsonic velocity. The test was conducted by maintaining constant stagnation conditions, rather than a constant mass flow. Future tests will incorporate mass flow measurements in these comparisons. Better thrust performance would be expected provided the aerodynamic design of the upstream part of the nozzle plug was improved.

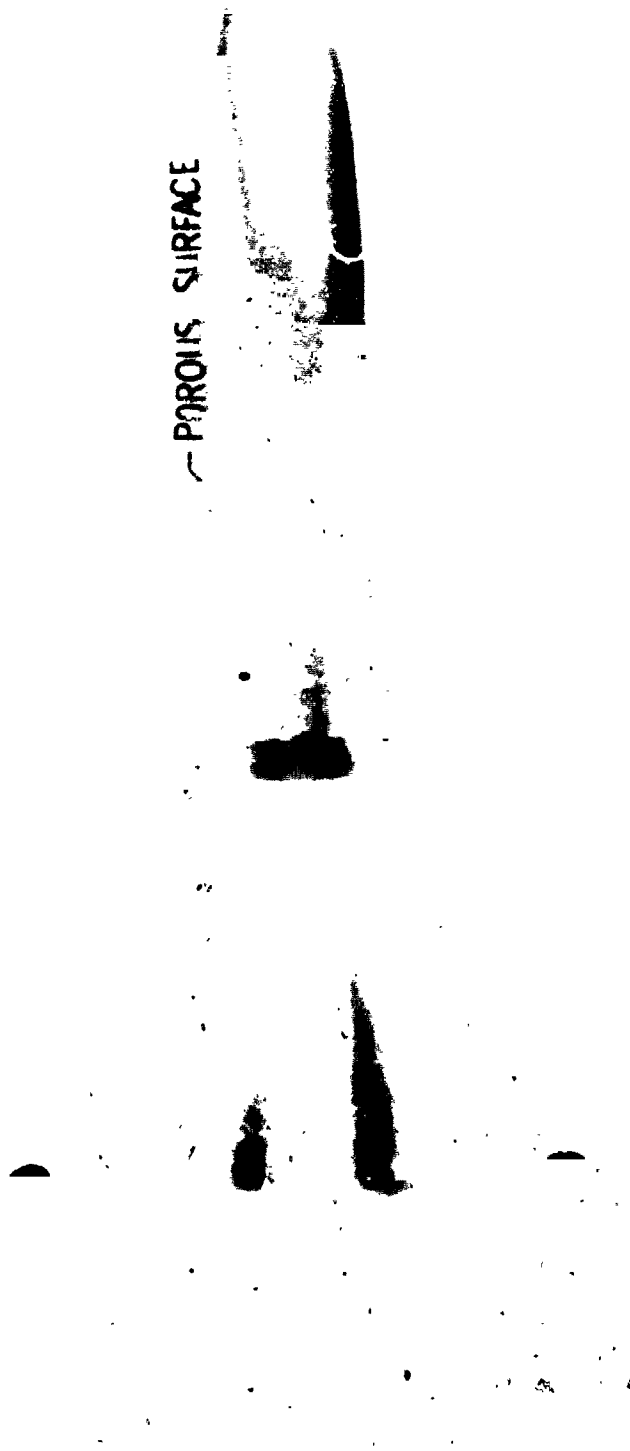
### CONCLUDING REMARKS

This paper contains a description of the configuration and operating characteristics of a porous center body plug nozzle jet noise suppressor that provides shock free flow over a wide range of nozzle pressure ratios. The elimination of the shocks and the resulting "shock associated noise" and "screeching" is accomplished by equilization of pressure along the jet axis. Because of the geometrical feature of the porous plug nozzle, shear noise reductions are also observed at all subsonic and supersonic flow conditions tested.

Additional benefits are the localization of the noise sources in the flow and the reduction of the spatial scale of the large structure of the jet flow, which enhance the performance of an acoustic baffle.

#### REFERENCES

1. Powell, A. On the Mechanism of Choked Jet Noise, Proceedings of the Physics Society, Vol. 66, pp. 1039-1056, 1953.
2. Harper-Bourne, M; and Fisher, M. J.; The Noise from Shock Waves in Supersonic Jets, Proceeding (No. 131), 1973 of the AGARD Conference on Noise Mechanisms.
3. Tanna, H. K., An Experimental Study of Jet Noise Part II: Shock Associated Noise, Journal of Sound and Vibration (1977), 50(3), pp. 429-444.
4. Howe, M. S. and Ffowcs Williams, On the Noise Generated By an Imperfectly Expanded Supersonic Jet, Philosophical Transactions of the Royal Society of London, Vol. 289, Number 1358, pp. (271-314) May 1978.
5. H. S. Ribner: Two Point Correlations of Jet Noise, Journal of Sound and Vibration, Vol. 56, No. 1, 1978, pp. (1-19), NASA TN D - 8330, 1976.
6. Lighthill, M. J., "On Sound Generated Aerodynamically, II Turbulence as a Source of Sound," Proc. Royal Society of London A, 222 (1954), pp. (1-32).
7. Lassister, L. W. and Hubbard, H. H.: Some Results of Experiments Relating to the Generation of Noise in Jets, J. Acoustic. Society of America Vol. 27, No. 3, May 1955, pp. 431-437.



— POROUS SURFACE

Figure 1.- Photograph of porous plug nozzle suppressor.

ORIGINAL PAGE IS  
OF POOR QUALITY

ORIGINAL PAGE IS  
OF POOR QUALITY



Figure 2.- Flow visualization at pressure ratio 3.72.

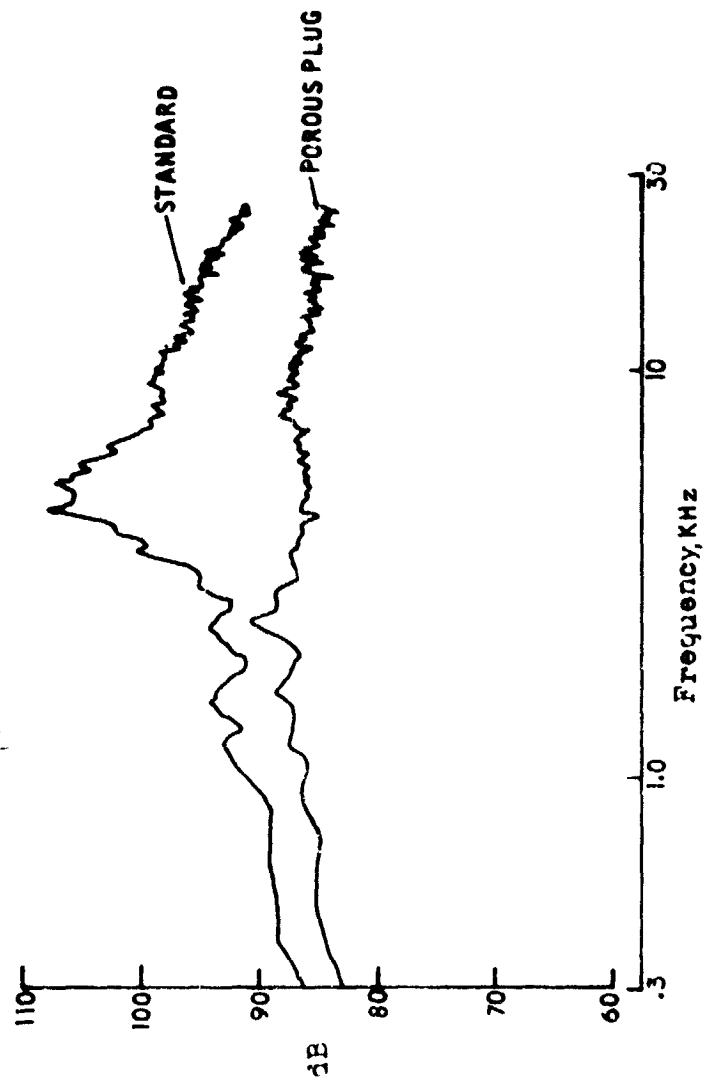


Figure 3.- Power spectral density of the far field pressure at 90° from jet axis at pressure ratio 3.72.

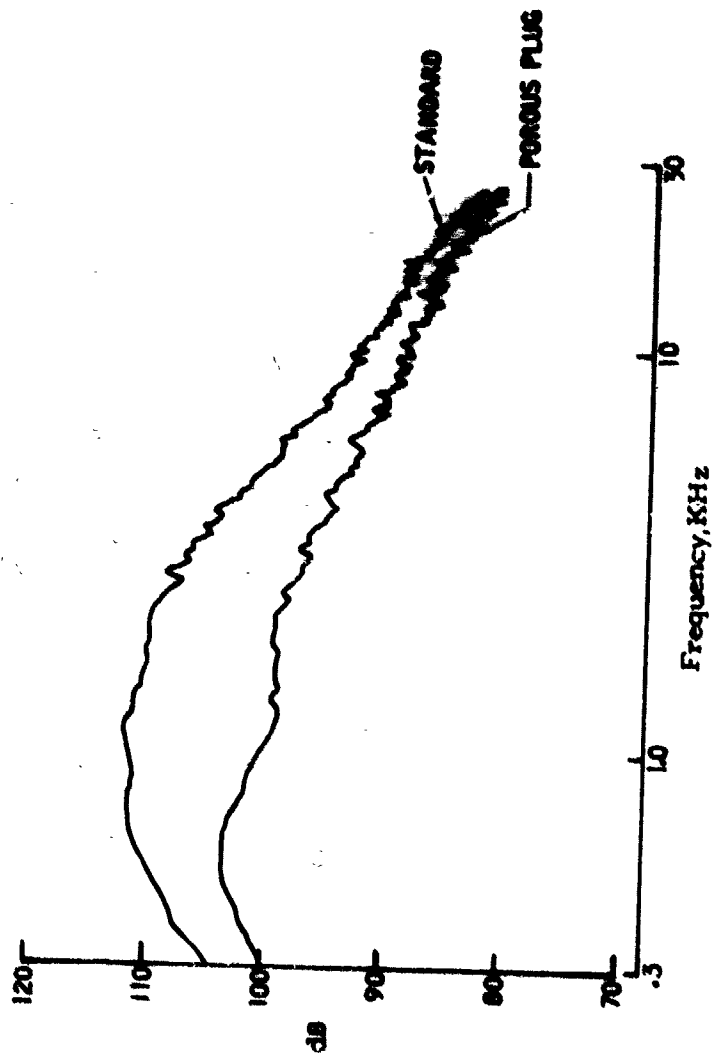


Figure 4.- Power spectral density of the far field pressure at 20° from jet axis at pressure ratio 3.72.



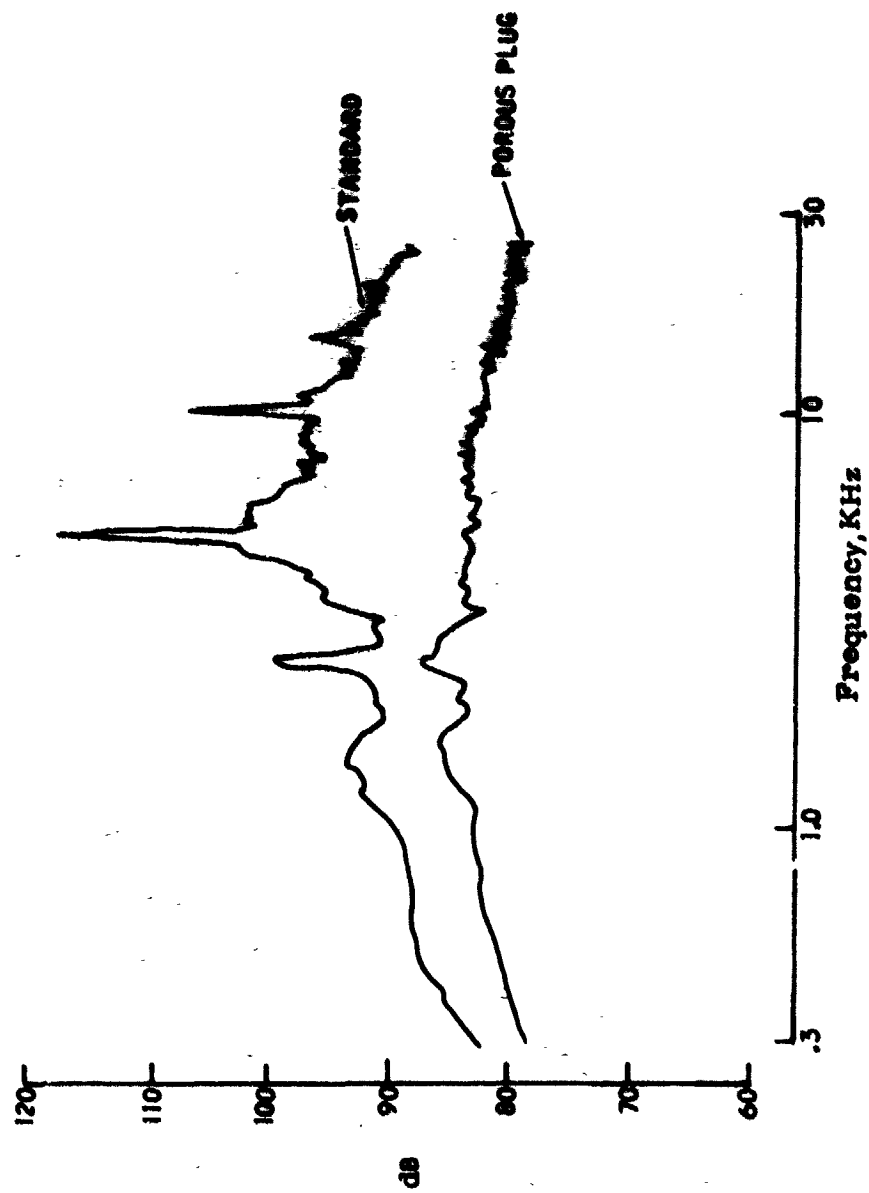


Figure 5.- Power spectral density of the far field pressure at 90° from jet axis at pressure ratio 3.04.

ORIGINAL PAGE IS  
OF POOR QUALITY

ORIGINAL PAGE IS  
OF POOR QUALITY

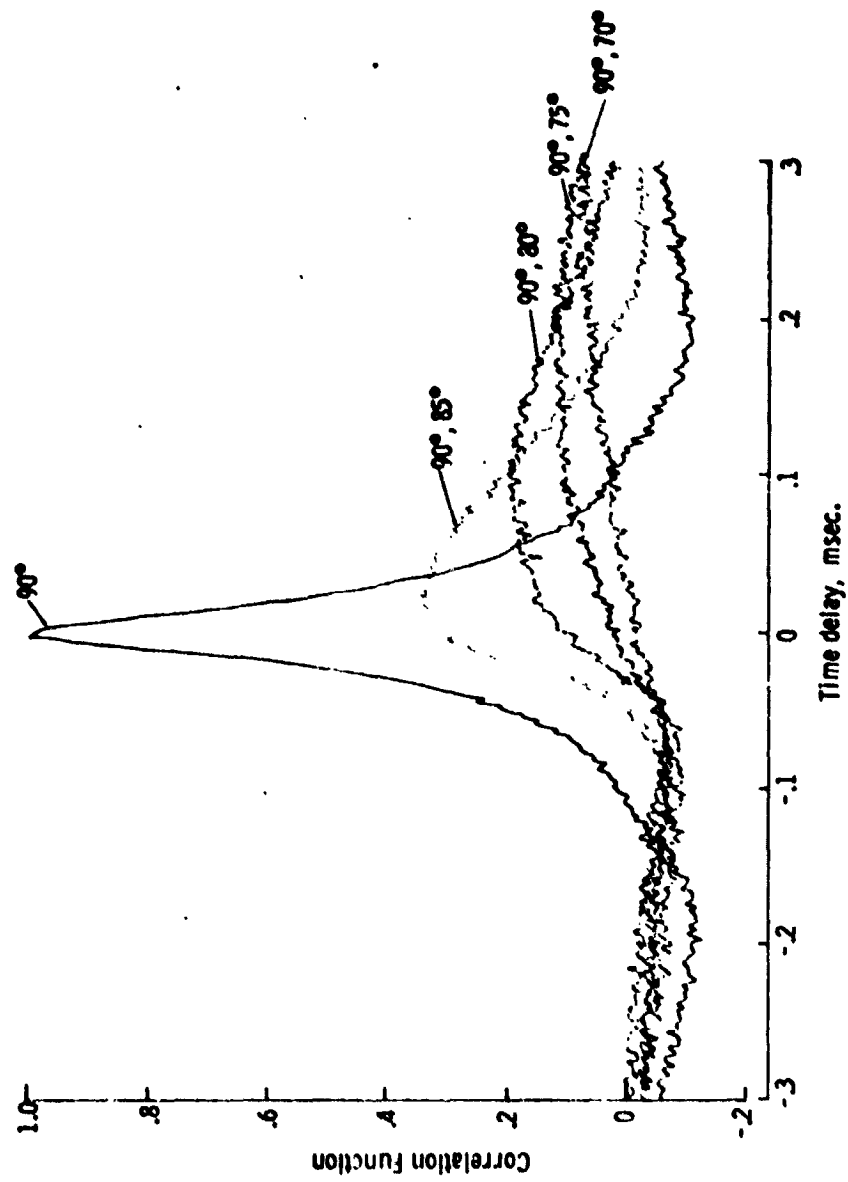


Figure 6.- Space time correlation of the far field pressure at 90° from jet axis  
for standard nozzle at pressure ratio 1.448.

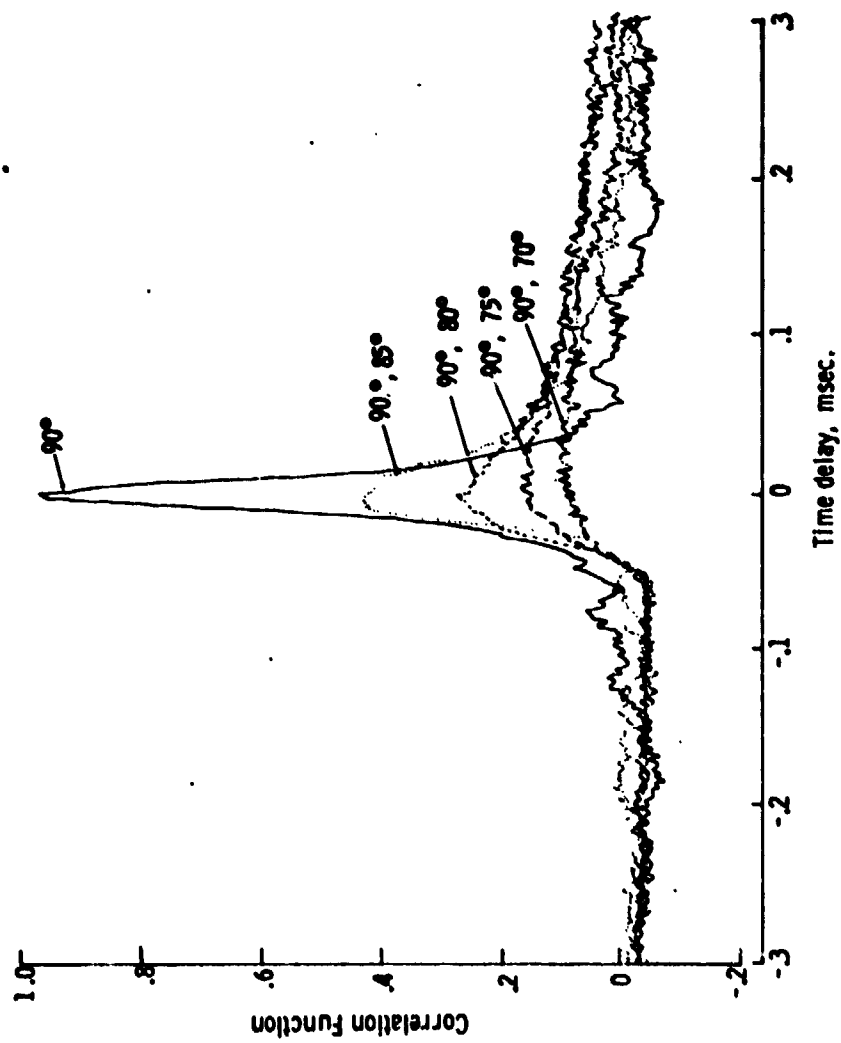


Figure 7.- Space time correlations of the far field pressure at 900 from jet axis for porous plug nozzle at pressure ratio 1.448.

ORIGINAL PAGE IS  
OF POOR QUALITY

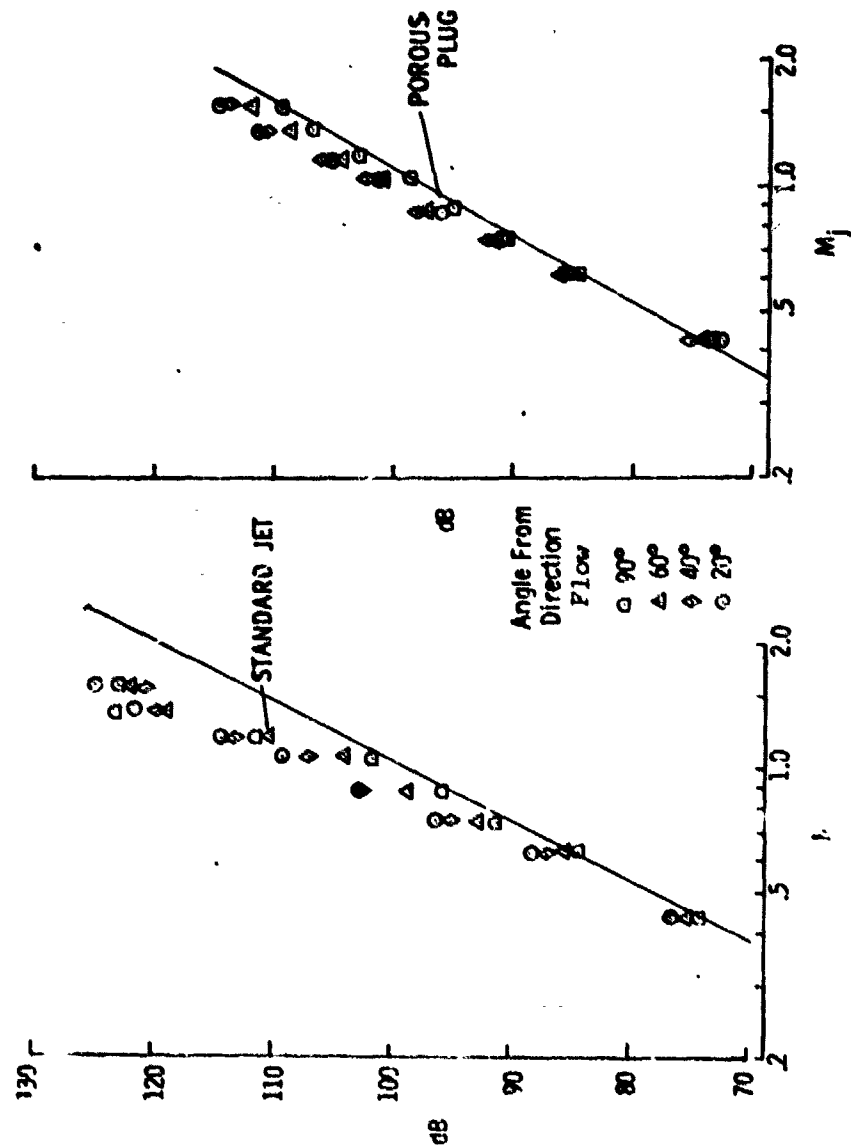


Figure 8.- Far field acoustic intensity.

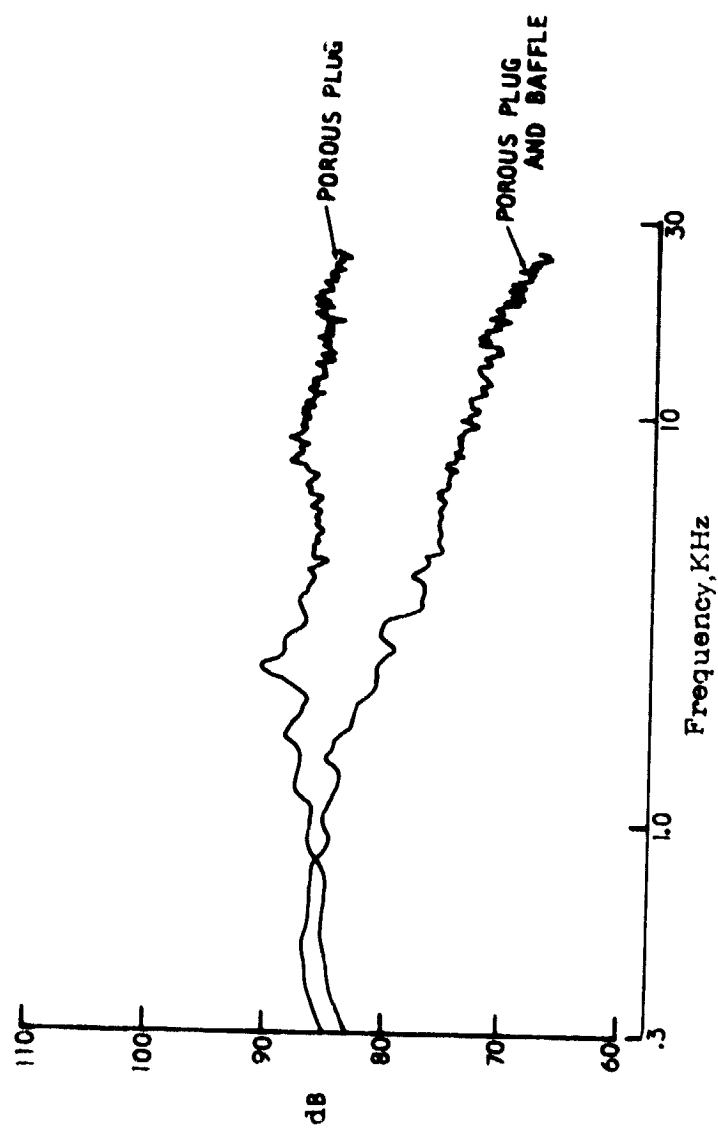


Figure 9.- Power spectral density of the far field pressure at 90° from jet axis at pressure ratio 3.72.